CARBON-NANOTUBE GEOMETRIES:
ANALYTICAL AND NUMERICAL RESULTS

Edoardo Mainini

Dipartimento di Ingegneria meccanica, energetica, gestionale
e dei trasporti (DIME), Università degli Studi di Genova,
Piazzale Kennedy 1, I-16129 Genova, Italy
& Faculty of Mathematics, University of Vienna,
Oskar-Morgenstern-Platz 1, A-1090 Vienna, Austria

Hideki Murakawa

Faculty of Mathematics, Kyushu University,
744 Motooka, Nishiku, Fukuoka, 819-0395, Japan

Paolo Piovano

Faculty of Mathematics, University of Vienna,
Oskar-Morgenstern-Platz 1, A-1090 Vienna, Austria

Ulisse Stefanelli

Faculty of Mathematics, University of Vienna,
Oskar-Morgenstern-Platz 1, A-1090 Vienna, Austria
& Istituto di Matematica Applicata e Tecnologie Informatiche "E. Magenes" - CNR,
v. Ferrata 1, I-27100 Pavia, Italy

(Communicated by the associate editor name)

Abstract. We investigate carbon-nanotubes under the perspective of geometry optimization. Nanotube geometries are assumed to correspond to atomic configurations which locally minimize Tersoff-type interaction energies. In the specific cases of so-called zigzag and armchair topologies, candidate optimal configurations are analytically identified and their local minimality is numerically checked. In particular, these optimal configurations do not correspond neither to the classical Rolled-up model [5] nor to the more recent polyhedral model [3]. Eventually, the elastic response of the structure under uniaxial testing is numerically investigated and the validity of the Cauchy-Born rule is confirmed.

1. **Introduction.** Carbon nanotubes are believed to be promising nanostructures for the development of innovative technologies ranging from next-generations electronics, to optics, mechanics, and pharmacology. The investigation of the mechanical properties of carbon nanotubes has been the object of a large number of experiments carried out with different techniques, ranging from transmission electron microscopy [12, 21] to atomic force microscopy [22]. Despite the large research activity on these nanostructures, the modeling of their fine geometry is still debated.

In fact, different geometric models for carbon nanotubes have been set forth by characterizing indeed the nanostructure by prescribing different atomic positions.

Intuitively, carbon nanotubes can be visualized as atomic configurations showing cylindrical symmetry. One can interpret them as the result of the rolling-up of a graphene strip (sometimes referred to as a *graphene nanoribbon*). More precisely, assume to be given the *hexagonal lattice* $\{pa+qb+rc \ : \ p,q \in \mathbb{Z}, \, r = 0,1\}$ with $a = (\sqrt{3},0)$, $b = (\sqrt{3}/2, 3/2)$, and $c = (\sqrt{3}, 1)$. To each vector (ℓ, m) for $\ell, \, m \in \mathbb{N}$, $\ell > 2$, we associate the *nanotube* obtained by identifying the atom x with $x + \ell a + mb$ for $\ell, \, m \in \mathbb{N}$. Nanotubes are called *zigzag* for $m = 0$, *armchair* for $m = \ell$, and *chiral* in all other cases, see Figure 1. We concentrate in the following on zigzag and armchair topologies, leaving the chiral case aside, for it involves additional intricacies.
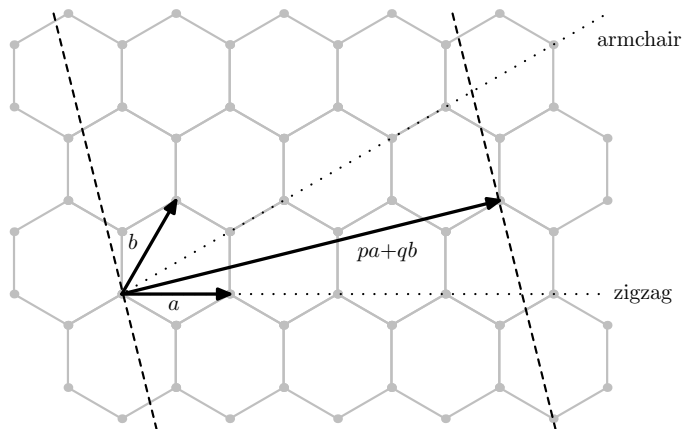

FIGURE 1. Rolling-up of nanotubes from a graphene sheet.

The purpose of this note is to comment on the possibility of describing nanotube geometries on a purely variational ground. In Section 2 we consider a phenomenological interaction energy of Tersoff type (see (2) and references [19, 20]) and we identify effective nanotube geometries as *stable* configurations, i.e., strict local energy minimizers. In Section 3 we begin by addressing the zigzag geometry and by observing that the minimization problem becomes one-dimensional if we reduce to specific classes of *objective structures* (see [7]). In Section 4 we analytically show its well-posedness (see Theorem 4.3). In Section 5 and Section 6 the same program is applied to the armchair geometry (see in particular Theorem 6.1). Finally, in Section 7 we present numerical evidence of the fact that the above-mentioned optimal configurations are indeed strict local minimizers of the energy with respect to general perturbations. An analytical discussion of this point is subject of the forthcoming [16]. The optimality of objective configurations is checked also in presence of prescribed-displacement boundary conditions. This corresponds to a numerical validation of the so-called *Cauchy-Born* assumption and delivers a quantitative description of the whole elastic response of the structure under uniaxial testing.

As already mentioned, a number of different continuum and atomistic models for zigzag and armchair nanotubes is already available in the literature. Among atomistic models, especially two have drawn the most of the attention. These are the classical *Rolled-up model*, introduced in [4, 5, 10], and the *Cox-Hill model* (also

known as *polyhedral* model) proposed in [3]. Both models assume that atoms are arranged on the surface of a cylinder, but differ in the prescription of the bond angles formed at each atom. In the Cox-Hill model all bond angles are assumed to be equal, hence smaller than $2\pi/3$ in order to allow for the nonplanarity of the structure. On the other hand, in the Rolled-up model some of these angles are set to be equal to $2\pi/3$ (precisely, one angle for the zigzag and two for the armchair topology, respectively).

In Proposition 4.1 and Proposition 4.2 we show that, under the generic assumptions on the interaction densities which are introduced in Section 2 below, neither the Rolled-up nor the Cox-Hill model are local minimizers of the energy in the zigzag case. The same is obtained for the armchair case in Theorem 6.1. These results are in accordance with the measurements carried on in [24] reporting indeed on the low accuracy of Rolled-up and Cox-Hill models for extremely thin nanotubes. Furthermore, experimental and computational (molecular dynamics) evidence that different bond angles (and different bond lengths) are needed to properly model these nanotubes is provided in [1, 2, 8, 9, 11, 13].

An extension of the Cox-Hill model to these situations has been considered in [14] where it is remarked that two bond angles can be expected to be equal in the armchair and in the zigzag geometry (while three different angles seem in general to be needed for modeling chiral nanotubes). This finds confirmation for a specific choice of the interaction energy in [17, 18, 23] where the contribution to the energy of a single carbon atom (plus the three nearest neighbors) is numerically investigated. We follow here a close path, but we numerically analyze the stability of the whole structure and, in addition, we provide some analytical results.

2. **Mathematical Setting.** Let us introduce the mathematical setting. Nanotubes are represented by *configurations* of atoms, i.e. collections of points in $\mathbb{R}^3$ representing the atomic sites. Since the length of nanotubes may be as long as 10^7 times their diameter, we are here not interested in describing the nanotube geometry close to their ends. Thus, we restrict to periodic configurations, i.e. configurations that are invariant with respect to a translation of a certain period in the direction of the nanotube axis. Without loss of generality we consider only nanotubes with axis in the $\mathbf{e}_3 := (0,0,1)$ direction. Therefore, a nanotube is identified with a configuration

$$\mathcal{C} := C_n + L\mathbf{e}_3\mathbb{Z}$$

where $L > 0$ is the *period* of $\mathcal{C}$ and $C_n := \{x_1, \ldots, x_n\}$ is a collection of n points $x_i \in \mathbb{R}^3$ such that $x_i \cdot \mathbf{e}_3 \in [0, L)$. In the following, we will refer to C_n as the *n-cell* of $\mathcal{C}$, and since $\mathcal{C}$ is characterized by its n-cell C_n and its period L, we will systematically identify the periodic configuration $\mathcal{C}$ with the couple (C_n, L), i.e. $\mathcal{C} = (C_n, L)$.

We now introduce *the configurational energy E of a nanotube $\mathcal{C}$*, and we detail the hypotheses assumed on E throughout the paper. The energy E is given by the sum of two contributions, respectively accounting for the *two and the three-body interactions among particles* that are respectively modulated by the potentials v_2 and v_3, see (2).

The *two-body potential* $v_2 : \mathbb{R}^+ \to [-1, \infty)$ is required to assume its minimum value -1 uniquely at 1. Moreover, we ask v_2 to be *short-ranged*, that is to vanish shortly after 1. For the sake of definiteness, let us define $v_2(r) = 0$ for $r > \rho$ with $\rho := 1.1$. We say that two particles $x, y \in \mathcal{C}$ are *bonded*, or that the bond between

x and y is *active*, if $|x - y| < \rho$, and we refer to the graph formed by all the active bonds as the *bond graph* of $\mathcal{C}$. By periodicity this translates in considering two particles x_i and x_j of the n-cell C_n of $\mathcal{C}$ as bonded if $|x_i - x_j|_L < \rho$ where $|\cdot|_L$ is the *distance modulo L* defined by

$$|x_i - x_j|_L := \min_{z \in \{-1, 0, +1\}} |x_i - x_j + Lz\mathbf{e}_3|$$

for every $x_i, x_j \in C_n$. Let us denote by $\mathcal{N}$ the set of all couples of indexes corresponding to bonded particles, i.e.

$$\mathcal{N} := \{(i,j) \, : \, x_i, \, x_j \in C_n, \, i \neq j, \text{ and } |x_i - x_j|_L < \rho\},$$

and by x_i^j the particle in $\{x_i + Lz\mathbf{e}_3 \, : \, z = -1, 0, +1\}$ such that $|x_i^j - x_j| = |x_i - x_j|_L$.

The *three-body potential* $v_3 : [0, 2\pi) \to [0, \infty)$ is assumed to be symmetric around π, namely $v_3(\alpha) = v_3(2\pi - \alpha)$, and to be taking its minimum value 0 only at $2\pi/3$ and $4\pi/3$. The potential v_3 is also assumed to be convex and strictly decreasing in the interval

$$I_\varepsilon := (2\pi/3 - \varepsilon, 2\pi/3], \tag{1}$$

for some $\varepsilon < \pi/8$. Moreover, v_3 is required to be differentiable at each point of I_ε, so that in particular $v_3'(2\pi/3) = 0$. The choice of ε is arbitrary. Small values of ε correspond to a weaker assumption on the potential but will force us to restrict to large diameter tubes during the analysis, namely large values of ℓ. In turn, minimal tube diameters can be discussed by assuming ε to be relatively large.

The configurational energy E of a nanotube $\mathcal{C} = (C_n, L)$ is defined by

$$E(\mathcal{C}) = E(C_n, L) := \frac{1}{2} \sum_{(i,j) \in \mathcal{N}} v_2(|x_i - x_j|_L) + \frac{1}{2} \sum_{(i,j,k) \in \mathcal{T}} v_3(\alpha_{ijk}) \tag{2}$$

where the angle α_{ijk} refers to the angle formed by the vectors $x_i^j - x_j$ and $x_k^j - x_j$ (clockwise measured from x_i^j to x_k^j), see Figure 2 , and the index set $\mathcal{T}$ to the triples corresponding to first-neighboring particles, i.e.

$$\mathcal{T} := \{(i,j,k) \, : \, i \neq k, \, (i,j) \in \mathcal{N} \text{ and } (j,k) \in \mathcal{N}\}.$$

For all triples $(i,j,k) \in \mathcal{T}$ we call α_{ijk} a *bond angle*.

We observe that the above assumptions are generally satisfied by classical interaction potentials for carbon (see [19, 20]). In particular, note that we are not imposing here that the two-body potential v_2 is repulsive at short-range although this is a fairly classical assumption and, currently, the only frame in which crystallization in the hexagonal lattice has been rigorously proved [6, 15].

Note that in Section 7 a specific energy that satisfies these hypotheses is considered for the numeric simulations, see (23) and (24).

Since the energy E is clearly rotation and translation invariant, in the following we will tacitly assume that all statements are to be considered up to isometries. We say that a nanotube $\mathcal{C} = (C_n, L)$ is *stable* if (C_n, L) is a local minimizer of the interaction energy E.

3. **Zigzag carbon nanotube geometry.** We begin by modeling zigzag nanotubes, armchair geometry being described later in Section 5 instead.

By prescribing the position of the atoms on each nanotube section we introduce a one-dimensional family of zigzag configurations $\mathscr{F}_z$ that will play a crucial role, as already mentioned in the Introduction. These configurations are indeed *objective*, in the sense of [7], as they are obtained as orbits of a finite set of atoms under the
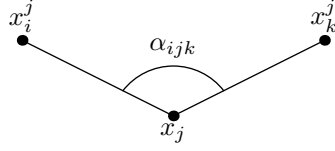
FIGURE 2. Notation for bonds and bond angles.

action of a prescribed isometry group. In particular, we fix the integer $\ell > 3$ and define the family $\mathscr{F}_z$ as the collection of all configurations that, up to isometries, coincide with

$$\left\{ \left(r \cos\left(\frac{\pi(2i+k)}{\ell}\right), r\sin\left(\frac{\pi(2i+k)}{\ell}\right), k(1+s)+j \right) \; \middle| \right. \tag{3}$$
$$\left. i = 1, \ldots, \ell, \; j = 0, 1, \; k \in \mathbb{Z} \right\}$$

for some choice of

$$r \in \left(0, \frac{1}{2\sin(\pi/(2\ell))}\right) \quad \text{and} \quad s \in (0, 1)$$

such that

$$s^2 + 4r^2 \sin^2\left(\frac{\pi}{2\ell}\right) = 1. \tag{4}$$

$\mathscr{F}_z$ is therefore a one-parameter smooth family of configurations, as each configuration in $\mathscr{F}_z$ is uniquely determined by r or s, taking relation (4) into account. An illustration of a configuration in $\mathscr{F}_z$ is in Figure 3 below.
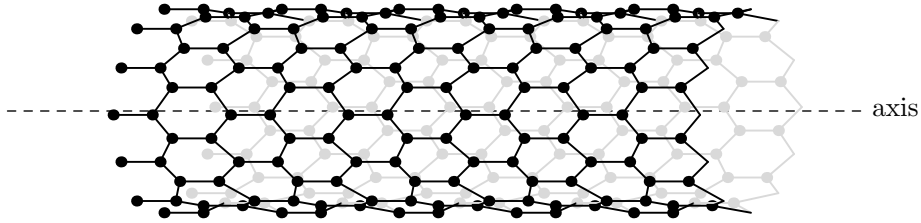

FIGURE 3. Zigzag nanotube.

The following basic geometric properties hold.

Proposition 3.1. *Let $\mathcal{F} \in \mathscr{F}_z$. Then*

(a) *Atoms in $\mathcal{F}$ lie on the surface of a cylinder whose radius is r and whose axis direction is $\boldsymbol{e}_3$.*

(b) *Atoms in $\mathcal{F}$ are arranged in planar sections, perpendicular to $\boldsymbol{e}_3$, obtained by fixing k and j in (3). Each of the sections exactly contains ℓ atoms, arranged as the vertices of a regular ℓ-gon. For each section, the two closest sections are at distance s and 1, respectively.*

(c) *The configuration $\mathcal{F}$ is invariant under a rotation of $2\pi/\ell$ around $\boldsymbol{e}_3$, under the translation $2(1+s)\boldsymbol{e}_3$, and under a rototranslation of angle π/ℓ along the vector $(1+s)\boldsymbol{e}_3$.*

(d) *Let $i \in \{1, \dots, \ell\}$, $k \in \mathbb{Z}$ and $j \in \{0, 1\}$: the triple (i, k, j) individuates points of $\mathcal{F}$. Given $x \equiv (i, k, 0) \in \mathcal{F}$, the three points $(i, k, 1)$, $(i, k-1, 1)$ and $(i-1, k-1, 1)$ have distance 1 from x. Similarly, if $x \equiv (i, k, 1)$, the distance of x from $(i, k, 0)$, from $(i, k+1, 0)$ and from $(i-1, k+1, 0)$ is 1. Here $(0, k, j)$ identifies with (ℓ, k, j).*

Proof. All the assertion are straightforward consequences of the definition. In particular, at each $x \in \mathcal{F}$, by triggering j we obtain another point at distance 1, the bond being parallel to $\mathbf{e}_3$. The other two points at distance 1 are obtained from x with a rotation of π/ℓ around $\mathbf{e}_3$ (one for each sense) and then with a translation of s in the direction of $\mathbf{e}_3$. Therefore they both have square distance from x equal to $4r^2 \sin^2(\pi/(2\ell)) + s^2$, which is equal to 1 by (4), and they minimize the distance from x among the other points on the same section.   □

Notice that the parameters range between two degenerate cases: $r = 0$ (the cylinder is reduced to its axis) and $s = 0$ (sections collide). However, we shall impose further restrictions because each atom should have three (active) bonds in order to represent a carbon nanotube. In particular, the only three bonds per atom should be the ones individuated by point (d) of Proposition 3.1. By recalling that two particles are bonded if their distance is less than the reference value 1.1, since the distance between two consecutive sections is either 1 or s, we require $s > 1/20$, i.e. $r < r_z^+ := \sqrt{0.9975}/(2\sin(\pi/(2\ell)))$. On the other hand, on each section, the edge of the regular ℓ-gon should be greater than 1.1. Such length is given by $2r \sin\gamma_\ell$, where γ_ℓ is the internal angle of a regular 2ℓ-gon, i.e.

$$\gamma_\ell := \pi \left(1 - \frac{1}{\ell}\right). \tag{5}$$

Therefore, we need to impose $r > r_z^- := 0.55/\sin\gamma_\ell$. With these restrictions we have the following

Proposition 3.2. *Let $\mathcal{F} \in \mathscr{F}_z$ with $r_z^- < r < r_z^+$. Then, all atoms in $\mathcal{F}$ have exactly 3 (first-nearest) neighbors, at distance 1, with one bond in the direction of $\mathbf{e}_3$. Among the corresponding three smaller than π bond angles, two have amplitude α (the ones involving atoms in three different sections), and the third has amplitude β_z, where $\alpha \in (\pi/2, \pi)$ is obtained from*

$$\sin\alpha = \sqrt{1 - s^2} = 2r \sin\left(\frac{\pi}{2\ell}\right) \tag{6}$$

and β_z is given by

$$\beta_z = \beta_z(\alpha) := 2\arcsin\left(\sin\alpha \sin\frac{\gamma_\ell}{2}\right). \tag{7}$$

Proof. The restrictions on r imply that there are three (unit length) bonds per atom, as seen in the above discussion. The amplitude of the three corresponding active bond angles do not depend on the atom: this follows from property (c) in Proposition 3.1. The value of α is obtained by elementary trigonometry, indeed $\alpha = \widehat{ABC} = \widehat{ABD}$ from Figure 3, where B represents a point of $\mathcal{F}$, surrounded by its three first neighborhoods. We have $\overline{CR} = \overline{BC} \sin\alpha$ since $\widehat{BRC} = \pi/2$. Hence, we compute that

$$\overline{CD} = 2\overline{CR} \sin(\gamma_\ell/2) = 2\overline{BC} \sin\alpha \, \sin(\gamma_\ell/2). \tag{8}$$

Now, relation (7) follows from (8) since $\overline{BC} = \overline{BD} = 1$ and $\beta_z(\alpha) = \widehat{CBD}$.   □
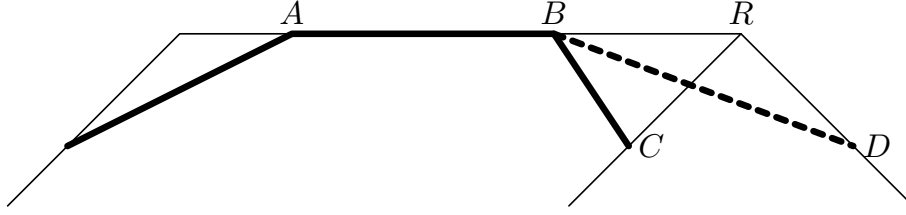
FIGURE 4. The construction of the function β_z.
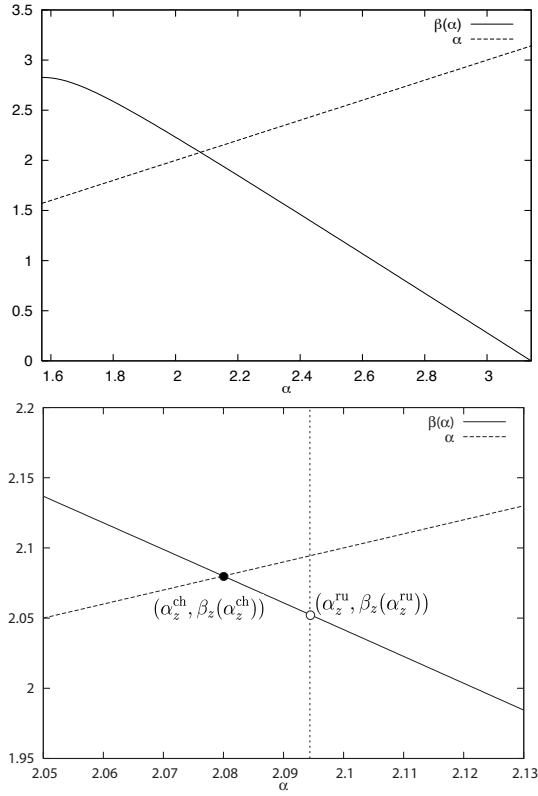
FIGURE 5. The angle β_z as a function of the angle α (above) and a zoom (below) with the points $(\alpha_z^{\mathrm{ru}}, \beta_z(\alpha_z^{\mathrm{ru}}))$ and $(\alpha_z^{\mathrm{ch}}, \beta_z(\alpha_z^{\mathrm{ch}}))$ for $\ell = 10$.

As already mentioned, the nice feature of the collection $\mathscr{F}_z$ is that all its configurations are smoothly and uniquely determined by the specification of a single scalar parameter. Among the equivalent choices for such a parameter, we concentrate from now on the bond angle α, which is introduced in Proposition 3.2, instead of the parameters r or s appearing in the definition of $\mathscr{F}_z$. The relation among the three is given by (6). In particular, the constraint corresponding to $r < r_z^+$ is $\alpha > \alpha_z^- := \arccos(-1/20) \approx 93°$ and the one corresponding to $r > r_z^-$ is $2\sin\alpha\sin(\gamma_\ell/2) > 1.1$ (notice that a constraint working for any $\ell \geq 4$ is $\alpha < \alpha_z^+ := \pi - \arcsin(1.1/\sqrt{2 + \sqrt{2}}) \approx 143.5°$). It follows from Proposition 3.2 that

for all $\alpha \in (\alpha_z^-, \alpha_z^+)$ we have exactly one configuration $\mathcal{F}_\alpha \in \mathscr{F}_z$, featuring 2/3 of the (smaller than π) bond angles of value α. Since the three angles at each atom of $\mathcal{F}_\alpha$ necessarily fulfill the elementary constraint

$$\beta_z + 2\alpha < 2\pi, \tag{9}$$

we have that the function β_z (introduced in (7) and defined in $(\pi/2, \pi)$) satisfies $\beta_z(\alpha) \in (0, 2(\pi - \alpha))$, see Figure 5. One explicitly computes that

$$\beta_z'(\alpha) = \frac{2 \sin \dfrac{\gamma_\ell}{2} \cos \alpha}{\sqrt{1 - \sin^2 \alpha \sin^2 \dfrac{\gamma_\ell}{2}}} < 0, \quad \beta_z''(\alpha) = -\frac{2 \sin \alpha \sin \dfrac{\gamma_\ell}{2} \cos^2 \dfrac{\gamma_\ell}{2}}{\left(1 - \sin^2 \alpha \sin^2 \dfrac{\gamma_\ell}{2}\right)^{3/2}} < 0 \tag{10}$$

for every $\alpha \in (\pi/2, \pi)$. Thus, β_z is strictly decreasing and strictly concave on (α_z^-, α_z^+).

Rolled-up and Cox-Hill zigzag models. The configurations corresponding with the Rolled-up and the Cox-Hill models (henceforth indicated as Rolled-up and Cox-Hill configurations) are included in the collection $\mathscr{F}_z$ along with the choices $\alpha = \alpha_z^{\mathrm{ru}} := 2\pi/3$ and $\alpha = \alpha_z^{\mathrm{ch}}$, respectively. The latter α_z^{ch} is the unique solution of the equation

$$\beta_z(\alpha_z^{\mathrm{ch}}) = \alpha_z^{\mathrm{ch}} \tag{11}$$

which exists as β_z is smooth and strictly decreasing in (α_z^-, α_z^+) from (10), $\beta_z(3\pi/5) > 3\pi/5$, and $\beta_z(2\pi/3) < 2\pi/3$, see Figure 5. Actually, the value α_z^{ch}, which is obviously smaller than α_z^{ru}, can be explicitly computed: indeed, using the definition (7), equation (11) has the solution

$$\alpha_z^{\mathrm{ch}} = \arccos \left(\frac{1 - 2\sin^2(\gamma_\ell/2)}{2\sin^2(\gamma_\ell/2)} \right),$$

which is approximately 114.5° for $\ell = 4$ and tends to $2\pi/3$ as $\ell \to \infty$.

4. **Minimizing the energy on $\mathscr{F}_z$.** Of course, a configuration $\mathcal{F}_\alpha$ in the family $\mathscr{F}_z$ is periodic. Its *minimal* period is explicit and depending on α, reading

$$\lambda_\alpha := 2(1 - \cos \alpha) = 2(1 + s).$$

Correspondingly, given $n = 4\ell$, the n-cell of $\mathcal{F}_\alpha = (F_\alpha, \lambda_\alpha)$ is given by the configuration F_α consisting of the $n = 4\ell$ points $x_i \in \mathcal{F}_\alpha$ such that $x_i \cdot \mathbf{e}_3 \in [0, \lambda_\alpha)$, i.e. the points on 4 consecutive sections. In particular, the energy $E(\mathcal{F}_\alpha)$ is the energy of the corresponding n-cell F_α, computed by means of (2) with respect to the minimal period λ_α. The energy on the family $\mathscr{F}_z$ hence reads

$$E(\mathcal{F}_\alpha) = E(F_\alpha, \lambda_\alpha) = -\frac{3n}{2} + n\widehat{E}_z(\alpha).$$

The first term in the above right-hand side is nothing but the two-body energy contribution and it is independent of α. On the other hand, the *zigzag angle energy* $\widehat{E}_z$ is defined by

$$\widehat{E}_z(\alpha) := v_3(\beta_z(\alpha)) + 2v_3(\alpha) \tag{12}$$

and represents the three-body energy contribution given by each atom of $\mathcal{F}_\alpha$. Hence, we have that

$$\mathcal{F}_\alpha \text{ minimizes } E \text{ on } \{\mathcal{F}_\alpha \in \mathscr{F}_z \,|\, \alpha \in A\} \iff \alpha \text{ minimizes } \widehat{E}_z \text{ on } A,$$

for an interval $A \subset (\alpha_z^-, \alpha_z^+)$. We wish to choose a suitable interval around the reference value $2\pi/3$. It shall depend on the number $\varepsilon \in (0, \pi/8)$ which is fixed from

the beginning, and corresponds to the choice of the interval I_ε where assumptions on v_3 are imposed, see (1). We first observe that, by recalling (7), $\beta_z > 2\pi/3 - \varepsilon$ is equivalent to

$$\alpha < \pi - \arcsin\left(\frac{\sin(\pi/3 - \varepsilon/2)}{\sin(\gamma_\ell/2)}\right) =: \sigma_z^\varepsilon.$$

Notice that $\sigma_z^\varepsilon < \alpha_z^+$ since $\varepsilon < \pi/8$. Moreover, as σ_z^ε increases with ℓ, if we define ℓ_z^ε by

$$\frac{\sqrt{3}}{2}\sin\left(\frac{\pi}{2} - \frac{\pi}{2\ell_z^\varepsilon}\right) = \sin\left(\frac{\pi}{3} - \frac{\varepsilon}{2}\right),$$

we obtain $\sigma_z^\varepsilon > 2\pi/3$ as soon as $\ell > \ell_z^\varepsilon$. Therefore, we consider from now on a large enough number ℓ of atoms per section, i.e. we assume $\ell > 3 \vee \ell_z^\varepsilon$ (and smaller values of ε thus correspond to more severe restriction on ℓ). In this way, after defining

$$A_z^\varepsilon := \left(\frac{2\pi}{3} - \varepsilon, \sigma_z^\varepsilon\right),$$

we obtain that $\alpha \in A_z^\varepsilon$ implies $\beta_z > 2\pi/3 - \varepsilon$ and $\alpha_z^{\mathrm{ru}} = 2\pi/3 \in A_z^\varepsilon$. Moreover, we have $\alpha_z^{\mathrm{ch}} \in A_z^\varepsilon$ for any $\varepsilon \in (0, \pi/8)$ and $\ell > \ell_z^\varepsilon$ (indeed, β_z is strictly decreasing and $\beta(2\pi/3 - \varepsilon) > \beta(\sigma_z^\varepsilon) = 2\pi/3 - \varepsilon$, therefore $\beta_z(\alpha_z^{\mathrm{ch}}) = \alpha_z^{\mathrm{ch}}$ implies $\alpha_z^{\mathrm{ch}} > 2\pi/3 - \varepsilon$). As a consequence, A_z^ε is an open neighborhood of the interval $(\alpha_z^{\mathrm{ch}}, \alpha_z^{\mathrm{ru}})$.

From here on $\varepsilon \in (0, \pi/8)$ and the integer $\ell > 3 \vee \ell_z^\varepsilon$ are fixed, and we shall perform the local minimization of the energy. We start by providing two negative results.

Proposition 4.1. *The Cox-Hill zigzag configuration is not a critical point for the energy.*

Proof. Let us start by proving that $\beta_z' > -2$. Indeed, we easily check the chain of elementary equivalences

$$-2 < \beta_z'(\alpha) \iff -\cos\alpha \sin\frac{\gamma_\ell}{2} < \sqrt{1 - \sin^2\alpha \sin^2\frac{\gamma_\ell}{2}}$$

$$\iff \cos^2\alpha \sin^2\frac{\gamma_\ell}{2} < 1 - \sin^2\alpha \sin^2\frac{\gamma_\ell}{2}$$

$$\iff \sin^2\frac{\gamma_\ell}{2} < 1$$

which holds since $\gamma_\ell < \pi$ for every ℓ. By (12) we obtain that

$$\widehat{E}_z'(\alpha_z^{\mathrm{ch}}) = 2v_3'(\alpha_z^{\mathrm{ch}}) + v_3'(\alpha_z^{\mathrm{ch}})\beta_z'(\alpha_z^{\mathrm{ch}}) = v_3'(\alpha_z^{\mathrm{ch}})(2 + \beta_z'(\alpha_z^{\mathrm{ch}})) < 0 \qquad (13)$$

since $\beta_z(\alpha_z^{\mathrm{ch}}) = \alpha_z^{\mathrm{ch}}$ and $v_3'(\alpha_z^{\mathrm{ch}}) < 0$. Hence, α_z^{ch} is not a critical point of $\widehat{E}_z$ and the Cox-Hill configuration $\mathcal{F}_{\alpha_z^{\mathrm{ch}}}$ is not a critical point for the energy E on $\{\mathcal{F}_\alpha \in \mathscr{F}_z \mid \alpha \in A_z^\varepsilon\}$. A fortiori, $\mathcal{F}_{\alpha_z^{\mathrm{ch}}}$ is not a critical point of the energy E. $\square$

Proposition 4.2. *The Rolled-up zigzag configuration is not a critical point for the energy.*

Proof. We have already remarked that $\beta_z(\alpha) > 2\pi/3 - \varepsilon$ for $\alpha \in A_z^\varepsilon$, and with (9) this implies $\beta_z(2\pi/3) \in I_\varepsilon$. Then, it suffices to use the assumptions on v_3 and compute

$$\widehat{E}_z'(2\pi/3) = 2v_3'(2\pi/3) + v_3'(\beta_z(2\pi/3))\beta_z'(2\pi/3) = v_3'(\beta_z(2\pi/3))\beta_z'(2\pi/3) > 0. \quad (14)$$

Thus, $2\pi/3$ is not a critical point of $\widehat{E}_z$. Hence, the Rolled-up configuration $\mathcal{F}_{\alpha_z^{\mathrm{ru}}}$ is not a minimizer of the energy E on $\{\mathcal{F}_\alpha \in \mathscr{F}_z \,|\, \alpha \in A_z^\varepsilon\}$. A fortiori, $\mathcal{F}_{\alpha_z^{\mathrm{ru}}}$ is not a critical point for the energy E. $\qquad\square$

We now prove that $\widehat{E}_z$ admits a unique minimizer in A_z^ε.

Theorem 4.3. *On the interval A_z^ε, the energy $\widehat{E}_z$ admits a unique global minimizer α_z^*. Correspondingly, $\mathcal{F}_z^* := \mathcal{F}_{\alpha_z^*}$ is the unique minimizer of E on $\{\mathcal{F}_\alpha \in \mathscr{F}_z \,|\, \alpha \in A_z^\varepsilon\}$. In particular, $\alpha_z^* \in (\alpha_z^{\mathrm{ch}}, \alpha_z^{\mathrm{ru}})$.*

Proof. After recalling that α_z^{ch} and α_z^{ru} belong to A_z^ε, we first show that there is no minimizer of $\widehat{E}_z$ on the interval $A_z^\varepsilon \cap \{\alpha < \tilde\alpha\}$, where $\tilde\alpha$ is the angle realizing $\beta_z(\tilde\alpha) = 2\pi/3$. By the monotonicity properties (10) of β_z, $\tilde\alpha$ is the unique angle with this property and clearly $\tilde\alpha < \alpha_z^{\mathrm{ch}}$. If $\tilde\alpha \le 2\pi/3 - \varepsilon$ there is nothing to prove, otherwise let $\alpha \in (2\pi/3 - \varepsilon, \tilde\alpha)$, so that $\beta_z(\cdot)$, which is decreasing, belongs to $(2\pi/3, 2\pi/3 + 2\varepsilon)$, thus

$$\widehat{E}_z(\alpha) = 2v_3(\alpha) + v_3(\beta_z(\alpha)) > 2v_3(\tilde\alpha) = 2v_3(\tilde\alpha) + v_3(\beta_z(\tilde\alpha)) = \widehat{E}_z(\tilde\alpha),$$

since v_3 is strictly decreasing in I_ε and since $v_3 \ge 0$ and $v_3(2\pi/3) = 0$.

Similarly there is no minimizer of $\widehat{E}_z$ in $(2\pi/3, \sigma_z^\varepsilon)$. Indeed, for α in such interval we have $\beta_z \in I_\varepsilon$ (this comes from (9) and from the definition of σ_z^ε) and then again the monotonicity of $\beta_z(\cdot)$ and of v_3 entails

$$\widehat{E}_z(\alpha) = 2v_3(\alpha) + v_3(\beta_z(\alpha)) > v_3(\beta_z(2\pi/3)) = \widehat{E}_z(2\pi/3).$$

Eventually, if $\alpha \in (\tilde\alpha \vee (2\pi/3 - \varepsilon), 2\pi/3)$, then $\beta_z \in I_\varepsilon$: since the composition of v_3 (convex and strictly decreasing on I_ε) and β_z (strictly concave) is strictly convex, it follows from (12) that $\widehat{E}_z$ is strictly convex in $(\tilde\alpha \vee (2\pi/3 - \varepsilon), 2\pi/3)$. We use this strict convexity together with (13) and (14) to infer that

$$\widehat{E}_z'(\alpha) < \widehat{E}_z'(\alpha_z^{\mathrm{ch}}) < 0 < \widehat{E}_z'(\alpha_z^{\mathrm{ru}})$$

for any $\alpha \in (\tilde\alpha \vee (2\pi/3 - \varepsilon), \alpha_z^{\mathrm{ch}})$, and that there is a unique minimizer α_z^* of $\widehat{E}_z$ in A_z^ε, found in $(\alpha_z^{\mathrm{ch}}, \alpha_z^{\mathrm{ru}})$. $\qquad\square$

The optimal configuration $\mathcal{F}_z^*$ does not coincide neither with the Cox-Hill nor with the Rolled-up configuration and it is rather some intermediate configuration (intermediate in the sense of the parametrization via α). As such it qualifies as a new, variationally-based, geometric model for zigzag nanotubes. The configuration $\mathcal{F}_z^*$ is uniquely defined in $\mathscr{F}_z$. Its most striking feature is that it is locally stable with respect to perturbations, not necessarily restricted to the family $\mathscr{F}_z$ (see Section 7). This fact is particularly remarkable as it allows to rigorously justify the geometry of the $3n$-dimensional nanotube configuration moving from variational considerations in one dimension.

5. **Armchair geometry.** We now address the armchair nanotube geometry and observe that the program outlined in the previous two sections for the zigzag nanotube can be carried out analogously.

First of all we introduce a family $\mathscr{F}_a$ of specific armchair configurations as the union of sections consisting of a fixed even integer $\ell > 2$ of atoms. In each section the ℓ atoms are arranged by dividing them in two groups of $\ell/2$ atoms, and then placing the atoms of each group at the vertices of a regular $(\ell/2)$-gon.

More precisely, let $\ell > 2$ be an even integer and define the family $\mathscr{F}_a$ as the collection of all configurations that, up to isometries, coincide with

$$\left\{ \left(r\cos\left(\frac{2\pi}{\ell}(2i+k) + q_r j\right), r\sin\left(\frac{2\pi}{\ell}(2i+k) + q_r j\right), pk \right) \right. \left| \right.$$

$$\left. i = 1, \ldots, \ell/2, \ j = 0, 1, \ k \in \mathbb{Z} \right\}$$

(15)

for some

$$r \in \left(\frac{1}{2\sin(\pi/\ell)}, \frac{1}{2\sin(\pi/(2\ell))} \right) \quad \text{and} \quad p \in (0, 1)$$

such that

$$p^2 + 4r^2 \sin^2\left(\frac{\pi}{\ell} - \frac{q_r}{2}\right) = 1,$$

(16)

where

$$q_r := 2\arcsin\left(\frac{1}{2r}\right).$$

Therefore, $\mathscr{F}_a$ is a one-parameter smooth family of configurations. Let us collect some geometric properties which hold for all the elements of $\mathscr{F}_a$.

Proposition 5.1. *Let $\mathcal{F} \in \mathscr{F}_a$. Then,*

(a) *Atoms in $\mathcal{F}$ lie on the surface of a cylinder whose radius is r and whose axis direction is $\boldsymbol{e}_3$.*

(b) *Atoms in $\mathcal{F}$ are arranged in planar sections, perpendicular to $\boldsymbol{e}_3$, obtained by fixing k and in (15). Each of the sections exactly contains ℓ atoms, arranged as the vertices of two regular $(\ell/2)$-gons, which are rotated of an angle q_r with respect to each other. For each section, the two closest sections are both at distance p.*

(c) *The configuration $\mathcal{F}$ is invariant under a rotation of $4\pi/\ell$ around the axis $\boldsymbol{e}_3$, under the translation $2p\boldsymbol{e}_3$, and under a rototranslation of an angle $2\pi/\ell$ and the vector $p\boldsymbol{e}_3$.*

(d) *Let $i \in \{1, \ldots, \ell/2\}$, $k \in \mathbb{Z}$ and $j \in \{0, 1\}$. The triple (i, k, j) individuates points of $\mathcal{F}$. Given $x \equiv (i, k, 0) \in \mathcal{F}$, the three points $(i, k, 1)$, $(i, k-1, 1)$ and $(i-1, k+1, 1)$ have distance 1 from x. Similarly, if $x \equiv (i, k, 1)$, the distance of x from $(i, k, 0)$, from $(i, k+1, 0)$ and from $(i+1, k-1, 0)$ is 1. Here $(0, k, j)$ identifies with $(\ell/2, k, j)$.*

Proof. The properties are direct consequence of the definition. About point (d), notice that for $x \equiv (i, k, j)$, by triggering j we remain on the same section and rotate of an angle q_r, the corresponding chord having length 1 by definition. The other two points are obtained by skipping to each of the two sections at distance p, and rotating around $\mathbf{e}_3$ of an angle $2\pi/\ell - q_r$, so the distance is 1 thanks to (16). $\square$

The parameters range between the two limit cases $p = 0$ (i.e. $q_r = \pi/\ell$) and $p = 1$ (i.e. $q_r = 2\pi/\ell$), in the first sections collide and in the second one obtains a prism shape. As for the zigzag configuration, the parameters should be additionally constrained in order not to activate extra bonds. Since p is the distance between two consecutive sections we require $2p > 1.1$. This corresponds, from (16), to $2r\sin(\pi/\ell - q_r/2) < \sqrt{0.6975}$, which yields $r < r_a^+$, where r_a^+ denotes the unique positive solution of the corresponding equality (notice that the map $r \mapsto 2r\sin(\pi/\ell - q_r/2)$ is monotone increasing for $r > 1/2$, as $\ell \geq 4$, and taking values 0 and 1 at

extremes values of r). Moreover, on each section, consider the distance between two consecutive atoms, one from each of the two ($\ell/2$)-gons. Such distance is either $2r\sin(q_r/2)$, which is 1 and corresponds to a bond described in point (d) of Proposition 5.1, or $2r\sin(2\pi/\ell - q_r/2)$, and the latter shall be greater than 1.1. Thus, we impose $r > r_a^-$, where r_a^- is, similarly, the unique positive solution to $2r\sin(2\pi/\ell - q_r/2) = 1.1$ After fixing these constraints on r we obtain the following statement, whose proof follows again by trigonometry arguments.

Proposition 5.2. *Let $\mathcal{F} \in \mathscr{F}_a$ with $r_a^- < r < r_a^+$. Then, all atoms in $\mathcal{F}$ have exactly 3 (first-nearest) neighbors, at distance 1, one bond being orthogonal to e_3. Among the corresponding three smaller than π bond angles, two have amplitude α (the ones involving the bond which is orthogonal to e_3) and the third has amplitude β_a, where $\alpha \in (\pi/2, \gamma_\ell)$ is given by*

$$\cos\alpha = 2r\cos\gamma_\ell \sin\left(\frac{\pi}{\ell} - \frac{q_r}{2}\right) \tag{17}$$

and

$$\beta_a = \beta_a(\alpha) := 2\arccos\left(\frac{\cos\alpha}{\cos\gamma_\ell}\right). \tag{18}$$

Analogously to the zigzag family, also the elements of $\mathscr{F}_a$ are smoothly and uniquely determined by the bond angle $\alpha \in (\pi/2, \gamma_\ell)$. Moreover, using (17), the constraint $r < r_a^+$ is equivalent to $\cos^2\alpha < 0.6975\cos^2\gamma_\ell$, and a constraint working for any $\ell \geq 4$ is $\alpha < \alpha_a^+ := \arccos(-\sqrt{0.34875}) \approx 126°$. On the other hand, using the identity $2r\sin(2\pi/\ell - q_r/2) = 1 + 4r\cos(\pi/\ell)\sin(\pi/\ell - q_r/2)$ and (17), the constraint $r > r_a^-$ becomes $\alpha > \alpha_a^- := \arccos(-1/20) \approx 93°$.

The angle β_a, that is defined as a function of α on $(\pi/2, \gamma_\ell)$ by (18), is smaller than $2(\pi-\alpha)$ since the elementary constraint needs to be satisfied

$$\beta_a + 2\alpha < 2\pi. \tag{19}$$

Furthermore, β_a is strictly decreasing and strictly concave since

$$\beta_a'(\alpha) = -\frac{2\sin\alpha}{\sqrt{\cos^2\gamma_\ell - \cos^2\alpha}} < 0 \quad \text{and} \quad \beta_a''(\alpha) = \frac{2\cos\alpha\sin^2\gamma_\ell}{(\cos^2\gamma_\ell - \cos^2\alpha)^{3/2}} < 0 \tag{20}$$

for every $\alpha \in (\pi/2, \gamma_\ell)$, see Figure 6.

Rolled-up and Cox-Hill armchair models. In the interval (α_a^-, α_a^+), we find the two relevant angles corresponding to the rolled up model and the Cox-Hill model. The first is the angle α_a^{ru} that satisfies $\beta(\alpha_a^{\mathrm{ru}}) = 2\pi/3$, in particular using (18) we find

$$\alpha_a^{\mathrm{ru}} = \arccos\left(\frac{\cos\gamma_\ell}{2}\right). \tag{21}$$

On the other hand, the angle α_a^{ch} is such that $\beta_a(\alpha_a^{\mathrm{ch}}) = \alpha_a^{\mathrm{ch}}$, which reads, from (18), $2\cos^2\alpha_a^{\mathrm{ch}} - \cos^2\gamma_\ell\cos\alpha_a^{\mathrm{ch}} - \cos^2\gamma_\ell = 0$. The solution is

$$\alpha_a^{\mathrm{ch}} = \arccos\left(\frac{1}{4}\cos^2\gamma_\ell - \frac{1}{4}\sqrt{\cos^4\gamma_\ell + 8\cos^2\gamma_\ell}\right).$$

In particular we have $\alpha_a^{\mathrm{ru}} < \alpha_a^{\mathrm{ch}} < 2\pi/3$, with $\alpha_a^{\mathrm{ru}} \approx 110,5°$ and $\alpha_a^{\mathrm{ch}} \approx 113°$ for $\ell = 4$. Both the values tend to $2\pi/3$ as $\ell \to \infty$.

6. **Minimizing the energy on $\mathscr{F}_a$.** Any configuration in $\mathscr{F}_a$ is periodic. Indeed, given the even integer $\ell \geq 4$ and a corresponding configuration $\mathcal{F}_\alpha \in \mathscr{F}_a$, we may identify a *minimal* periodicity n-cell F_α, with $n = 2\ell$, the period being

$$\Lambda_\alpha := 2 \left(1 - \frac{\cos^2 \alpha}{\cos^2 \gamma_\ell} \right)^{1/2} = 2p.$$

The energy of the configuration $\mathcal{F}_\alpha$ is therefore

$$E(\mathcal{F}_\alpha) = E(F_\alpha, \Lambda_\alpha) = -\frac{3n}{2} + n\widehat{E}_a(\alpha),$$

where

$$\widehat{E}_a(\alpha) := v_3(\beta_a(\alpha)) + 2v_3(\alpha). \tag{22}$$

In particular, the energy is again localized as all atoms are the same, and

$$\mathcal{F} \text{ minimizes } E \text{ on } \{\mathcal{F}_\alpha \in \mathscr{F}_a \,|\, \alpha \in A\} \iff \alpha \text{ minimizes } \widehat{E}_a \text{ on } A,$$

for any interval $A \subset (\alpha_a^-, \alpha_a^+)$. The choice of the suitable interval of minimization, which should contain the significant angles, is necessarily depending on the number $\varepsilon \in (0, \pi/8)$ which defines I_ε in (1), as the behavior of v_3 is known in I_ε. A necessary condition is $\beta_a > 2\pi/3 - \varepsilon$, which, by means of (18), reads

$$\alpha \leq \arccos(\cos \gamma_\ell \cos(\pi/3 - \varepsilon/2)) =: \sigma_a^\varepsilon,$$

and notice that σ_a^ε increases with ℓ. Therefore, if we fix $\varepsilon \in (0, \pi/8)$, we choose $\ell > 3 \vee \ell_a^\varepsilon$ and set

$$A_a^\varepsilon := \left(\frac{2\pi}{3} - \varepsilon, \sigma_a^\varepsilon \wedge \alpha_a^+ \right),$$

where ℓ_a^ε is the unique value of ℓ such that

$$\cos \gamma_\ell \cos \left(\frac{\pi}{3} - \frac{\varepsilon}{2} \right) = -\frac{1}{2},$$

we indeed obtain that $2\pi/3 \in A_a^\varepsilon$ and that $\alpha \in A_a^\varepsilon \Rightarrow \beta_a > 2\pi/3 - \varepsilon$. Moreover, A_a^ε contains α_a^{ru} for $\ell > 3 \vee \ell_a^\varepsilon$. Indeed, the value α_a^{ru} increases with ℓ, therefore it is enough to verify that the value of α_a^{ru} for $\ell = \ell_a^\varepsilon$ is greater than $2\pi/3 - \varepsilon$, that is, invoking (21), we have to check that

$$\cos \left(\frac{\pi}{3} - \frac{\varepsilon}{2} \right) \cos \left(\frac{2\pi}{3} - \varepsilon \right) > -\frac{1}{4}$$

for $\varepsilon \in (0, \pi/8)$. But this holds true since there is equality at $\varepsilon = 0$ and the left hand side is increasing in this interval as easily checked.

In analogy to Section 4, we now introduce the variationally-based geometric model for the armchair nanotube by minimizing E over the family $\mathscr{F}_a$, and we verify that it differs from the Cox-Hill and the Rolled-up configurations.

In particular, for the next result we fix $\varepsilon \in (0, \pi/8)$ and take $\ell > 3 \vee \ell_a^\varepsilon$, so that the interval A_a^ε is an open neighborhood of $(\alpha_a^{\mathrm{ru}}, 2\pi/3)$.

Theorem 6.1. *The Rolled-up and Cox-Hill armchair configurations are not critical points of E. Moreover, $\widehat{E}_a$ admits a unique global minimizer α_a^* in the interval A_a^ε. Thus, $\mathcal{F}_a^* := \mathcal{F}_{\alpha_a^*}$ is the unique minimizer of E on $\{\mathcal{F}_\alpha \in \mathscr{F}_a \,|\, \alpha \in A_a^\varepsilon\}$. In particular, $\alpha_a^* \in (\alpha_a^{\mathrm{ru}}, \alpha_a^{\mathrm{ch}})$.*
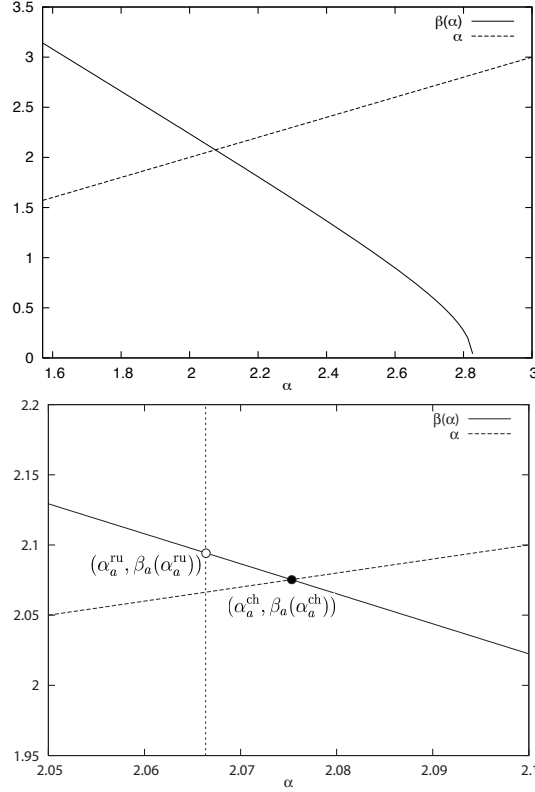
FIGURE 6. The angle β_a as a function of the angle α (above) and a zoom (below) with the points $(\alpha_a^{\mathrm{ru}}, \beta_a(\alpha_a^{\mathrm{ru}}))$ and $(\alpha_a^{\mathrm{ch}}, \beta_a(\alpha_a^{\mathrm{ch}}))$ for $\ell = 10$.

Proof. We begin by observing that the fact that the Rolled-up armchair configuration is not a critical point for the energy easily follows from the convexity and strict monotonicity of v_3 in I_ε and from $v_3'(2\pi/3) = 0$, that is

$$\widehat{E}_a'(\alpha_a^{\mathrm{ru}}) = 2v_3'(\alpha_a^{\mathrm{ru}}) + v_3'(2\pi/3)\beta_a'(\alpha_a^{\mathrm{ru}}) = 2v_3'(\alpha_a^{\mathrm{ru}}) < 0.$$

Furthermore, by the same argument used in Proposition 4.1 we have that also the Cox-Hill armchair configuration is not a critical point for the energy and that, in particular, $\widehat{E}_a'(\alpha_a^{\mathrm{ch}}) > 0$. In fact, from (20) it is easily seen that $\beta_a'(\alpha) < -2$. Hence, the same computation used in (13) this time shows that $\widehat{E}_a'(\alpha_a^{\mathrm{ch}}) > 0$.

We easily have $\widehat{E}_a(\alpha) > \widehat{E}_a(\alpha_a^{\mathrm{ru}})$ for $\alpha < \alpha_a^{\mathrm{ru}}$ and $\widehat{E}_a(\alpha) > \widehat{E}_a(2\pi/3)$ for $\alpha > 2\pi/3$, by the same arguments used in Theorem 4.3. We also have $\widehat{E}_a'(2\pi/3) = v_3'(\beta_a(2\pi/3))\beta_a'(2\pi/3) > 0$. These information, together with the fact that $\alpha \in (\alpha_a^{\mathrm{ru}}, 2\pi/3) \Rightarrow \beta_a \in I_\varepsilon$, so that reasoning as done in Theorem 4.3 $\widehat{E}_a$ turns out to be strictly convex in $(\alpha_a^{\mathrm{ru}}, 2\pi/3)$, entail that $\widehat{E}_a$ admits a unique minimizer in the interval A_a^ε. But we have seen that $\widehat{E}_a'(\alpha_a^{\mathrm{ch}}) > 0$ as well, therefore such a minimizer belongs to $(\alpha_a^{\mathrm{ru}}, \alpha_a^{\mathrm{ch}})$. $\qquad\square$

7. **Numerical investigation on stability.** The optimal geometries which have been identified above have been checked to be local energy minimizers within the

restricted class of highly-symmetric configurations $\mathscr{F}_a$ and $\mathscr{F}_z$, respectively. The aim of this section is to provide numerical evidence of the fact that they are indeed optimal with respect to generic small perturbations, possibly not restricted to $\mathscr{F}_a$ and $\mathscr{F}_z$. This entails that these optimal configurations are indeed strict local energy minimizers. We shall detail in [16] the analytical discussion of this problem and limit ourselves here in presenting the corresponding simulations.

7.1. **Minimization of the energy in $\mathscr{F}_a$ and $\mathscr{F}_z$.** We provide here an illustration to the analysis of the previous sections. Let us start by clarifying the simulation setting. The energy of the configuration $E = E_2 + E_3$ will be defined as in (2).

In all computations we prescribe the interaction energy densities as

$$v_2(r) = \begin{cases} f(r) - f(1.1) & \text{if } 0 < r < 1.1, \\ 0 & \text{otherwise} \end{cases} \tag{23}$$

$$f(r) = \frac{1}{2r^{12}} - \frac{1}{r^6},$$

$$v_3(\theta) = 10(\cos\theta + 1/2)^2. \tag{24}$$

In particular, note that v_2 is short-ranged and it is minimized uniquely at $r = 1$. Along with this provisions, we can immediately compute the energy $\widehat{E}_i$ along the corresponding family $\mathscr{F}_i$ for $i = a, z$, see Figure 7.

Notice that the above computation illustrates the already analytically proven fact that neither the *Rolled-up* angle α_i^{ru} nor the *Cox-Hill* angle α_i^{ch} are minimizers of the energy-per-particle $\widehat{E}_i$. On the contrary, one finds the optimal angles α_i^*. To these angles one associates the corresponding configurations in $\mathcal{F}_i^*$ which are hence global minimizers of the energy E in $\mathscr{F}_i$.

7.2. **Stability with respect to perturbations of the cell.** In order to provide numerical evidence of the fact that the optimal angles α_i^* ($i = z, a$) describe locally stable geometries, we compare energies of the optimal configurations $\mathcal{F}_i^*$ with those corresponding to perturbations.

As these perturbations may obviously brake the symmetry of the configuration, we are forced to work with the actual energy E instead of the simpler angle energies $\widehat{E}_i$. In particular, we need to specify the period L to be used for the computation of the energy $E(\cdot, L)$. Within this subsection, we fix this period to be $L_{\alpha_i^*}$, namely the period to be a suitable multiple of the minimal period of the optimal configurations $\mathcal{F}_i^*$. This amounts to say that we are considering perturbations of the n-cell of $\mathcal{F}_i^*$ only, leaving the period fixed. More general perturbations including changes in the period are considered in Subsection 7.3 below.

We shall fix the topology of the bond graph of the configurations under consideration. In order to check the robustness of our findings with respect to nanotubes of different aspect-ratios, we will concentrate on the following six topologies:

- Zigzag topologies:
  Z1) $\ell = 10$ atoms on the cross section, period $L = 4\lambda_{\alpha_z^*}$.
  Z2) $\ell = 20$ atoms on the cross section, period $L = 4\lambda_{\alpha_z^*}$.
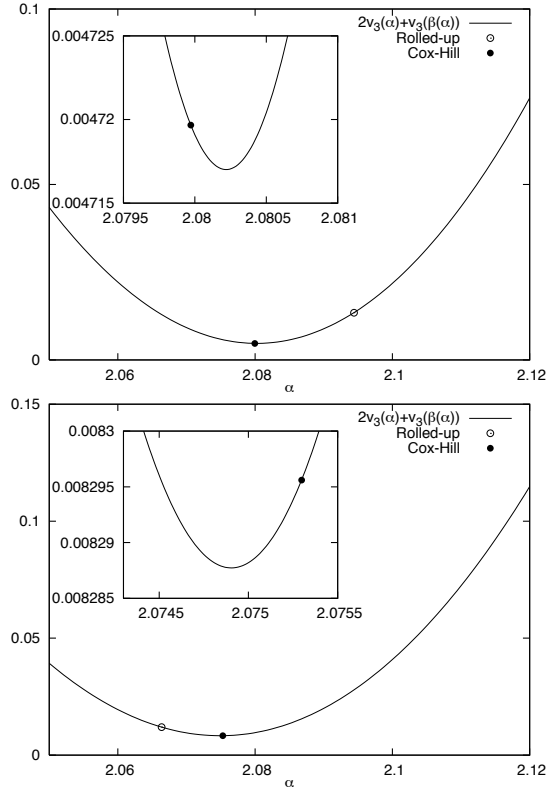 Z3) $\ell = 10$ atoms on the cross section, period $L = 8\lambda_{\alpha_z^*}$.
- Armchair topologies:
  A1) $\ell = 10$ atoms on the cross section, period $L = 4\Lambda_{\alpha_a^*}$.
  A2) $\ell = 20$ atoms on the cross section, period $L = 4\Lambda_{\alpha_a^*}$.
  A3) $\ell = 10$ atoms on the cross section, period $L = 8\Lambda_{\alpha_a^*}$.

FIGURE 7. The energy-per-particle $\widehat{E}_i$ in the zigzag (above) and in the armchair (below) family, as a function of the angle α for $\ell = 10$, together with a zoom about the minimum.

In all cases we generate random perturbations of the optimal cell $F_{\alpha_i^*}$ and compute the corresponding energy with respect to the given fixed period L. The results of the simulations are collected in Figure 8 and prove that indeed the optimal configurations are local strict energy minimizers.

7.3. **Stability with respect to general periodic perturbations.** We extend here the observations of Subsection 7.2 to the case of general periodic perturbations of the optimal $\mathcal{F}_i^*$ in $\mathscr{F}_i$. The point here is that the period of the configurations can also change in order to allow for noncompactly supported perturbations such as traction.

We focus here on the specific topology Z1, for definiteness, and identify

$$\mathcal{F}_z^* = (F_{\alpha_z^*}^*, L^*) \quad \text{for} \quad L^* = 4\lambda_{\alpha_z^*}$$

as the corresponding optimal configuration, along with its $n = 4(4\ell) = 160$-cell $F_{\alpha_z^*}^*$. Let now the period L be chosen in a small neighborhood of L^*. Correspondingly, let (F_L^*, L) be the only configuration in $\mathscr{F}_z$ with 160-cell F_L^* and period L. For different periods L, Figure 9 shows the comparison of the energy $E(F_L^*, L)$ with
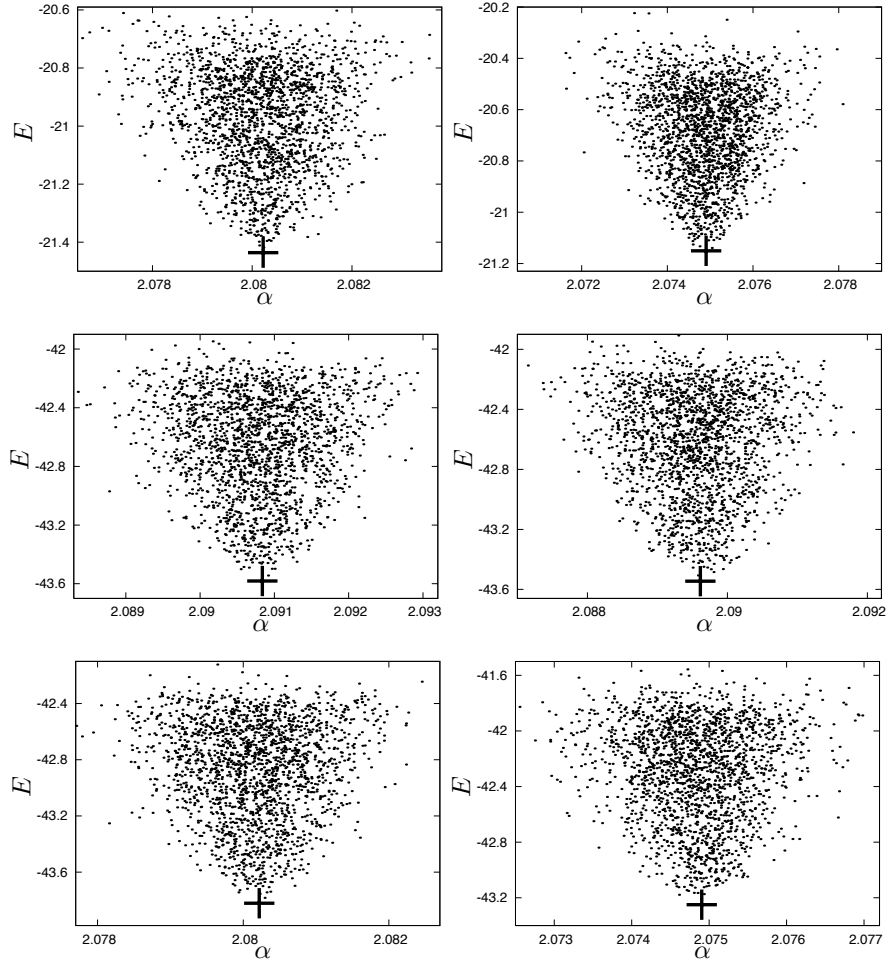
FIGURE 8. Comparison between energies of the optimal configurations and energies of their perturbations in the cases Z1, Z2, Z3 (left, from the top) and A1, A2, A3 (right, from the top). The marker corresponds to the optimal configuration $\mathcal{F}_i^*$ and value α represents the mean of all α-angles in the configuration.

that of random perturbations of the form $(\tilde{F}, L)$. The numerical evidence confirms that the optimal energy is reached by the configuration (F_L^*, L) for all given L.

These numerical results imply the stability of $(F_{\alpha_z^*}, L^*)$ with respect to general periodic perturbations. More precisely, we have the following

$$E\big(F_{\alpha_z^*}, L^*\big) \overset{\text{Thm. } 4.3}{\leq} E\big(F_L^*, L\big) \overset{\text{Figure } 9}{\leq} E(\tilde{F}, L)$$

for all perturbations $\tilde{F}$ of F_L^* where the first inequality is actually proved in Theorem 4.3.
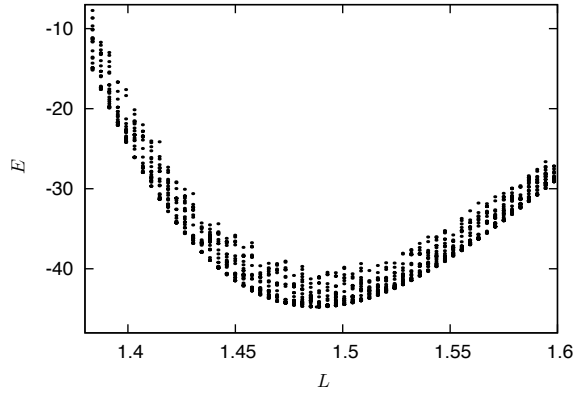
FIGURE 9. Optimality of the configuration $(F_L^*, L) \in \mathscr{F}_z$ (bottom point) for all given L in a neighborhood of L^*.
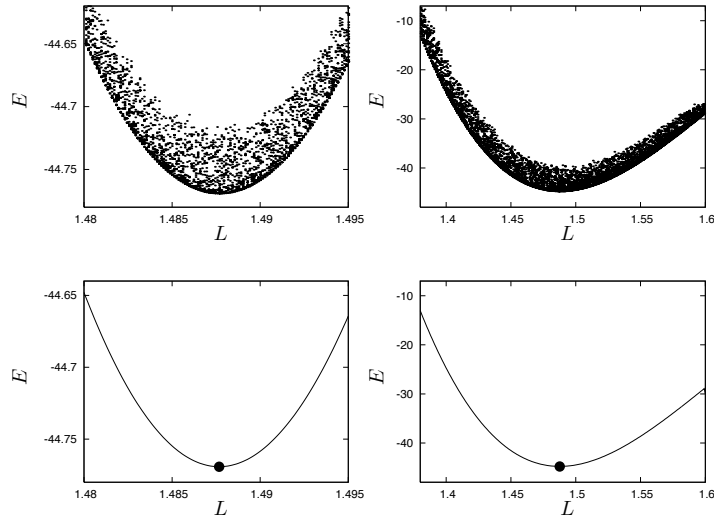

FIGURE 10. Elastic response of the nanotube Z1 under uniaxial small (left) and large displacements (right). The function $L \mapsto E(F_L^*, L)$ (bottom) corresponds to the lower envelope of the random evaluations (top).

These numerical findings actually provide a validation of the so-called *Cauchy-Born rule* under prescribed tensile displacement (hard device). Indeed, the Cauchy-Born rule can be formulated in this context as the optimality of (F_L^*, L) among all configurations with the same period. By directly computing $L \mapsto E(F_L^*, L)$ we

can describe the elastic response of the nanotube under tensile and compressive displacements, see Figure 10.

The nanotubes behaves linearly elastically in a neighborhood of the stress-free configuration $(F_{\alpha_i^*}, L^*)$. On the other hand, the mechanical response deviates from the linear elastic regime for strains of the order of 8%. This nonlinear behavior is both the effect of the specific shape of the two-body interaction potential in use and of the structure of the nanotube.

REFERENCES

[1] P. M. Agrawal, B. S. Sudalayandi, L. M. Raff, R. Komandur, Molecular dynamics (MD) simulations of the dependence of C-C bond lengths and bond angles on the tensile strain in single-wall carbon nanotubes (SWCNT), *Comp. Mat. Sci.* **41** (2008), 450–456.

[2] M. E. Budyka, T. S. Zyubina, A. G. Ryabenko, S. H. Lin, A. M. Mebel, Bond lengths and diameters of armchair single-walled carbon nanotubes, *Chem. Phys. Lett.* **407** (2005), 266–271.

[3] B. J. Cox, J. M. Hill, Exact and approximate geometric parameters for carbon nanotubes incorporating curvature, *Carbon*, **45** (2007), 1453–1462.

[4] M. S. Dresselhaus, G. Dresselhaus, R. Saito, Carbon fibers based on C_{60} ad their symmetry, *Phys. Rev. B*, **45** (1992), 11:6234–6242.

[5] M. S. Dresselhaus, G. Dresselhaus, R. Saito, Physics of carbon nanotubes, *Carbon*, **33** (1995), 883–891.

[6] W. E, D. Li, On the crystallization of 2D hexagonal lattices, *Comm. Math. Phys.* **286** (2009), 3:1099–1140.

[7] R. D. James, Objective structures, *J. Mech. Phys. Solids*, **54** (2006), 2354–2390.

[8] H. Jiang, P. Zhang, B. Liu, Y. Huans, P. H. Geubelle, H. Gao, K. C. Hwang, The effect of nanotube radius on the constitutive model for carbon nanotubes, *Comp. Mat. Sci.* **28** (2003), 429–442.

[9] V. K. Jindal, A. N. Imtani, Bond lengths of armchair single-walled carbon nanotubes and their pressure dependence, *Comp. Mat. Sci.* **44** (2008), 156–162.

[10] R. A. Jishi, M. S. Dresselhaus, G. Dresselhaus, Symmetry properties and chiral carbon nanotubes, *Phys. Rev. B*, **47** (1993), 24:166671–166674.

[11] K. Kanamits, S. Saito, Geometries, electronic properties, and energetics of isolated single-walled carbon nanotubes, *J. Phys. Soc. Japan*, **71** (2002), 2:483–486.

[12] A. Krishnan, E. Dujardin, T.W. Ebbesen, P.N. Yianilos, M.M.J. Treacy, Young?s modulus of single-walled nanotubes, *Phys. Rev. B* **58** (1998), 14013–14019

[13] J. Kurti, V. Zolyomi, M. Kertesz, G. Sun,The geometry and the radial breathing model of carbon nanotubes: Beyond the ideal behaviour, *New J. Phys*, **5** (2003), 125.1–21.

[14] R. K. F. Lee, B. J. Cox, J. M. Hill, General rolled-up and polyhedral models for carbon nanotubes, *Fullerenes, Nanotubes and Carbon Nanostructures*, **19** (2011), 88:726–748.

[15] E. Mainini, U. Stefanelli, Crystallization in carbon nanostructures, *Comm. Math. Phys.* **328** (2014), 2:545–571.

[16] E. Mainini, H. Murakawa, P. Piovano, U. Stefanelli. Carbon-nanotube geometries as optimal configurations. In preparation, 2015.

[17] L. Shen, J. Li, Transversely isotropic elastic properties of single-walled carbon nanotubes, *Phys. Rev. B* **69** (2004), 045414, Erratum *Phys. Rev. B* **81** (2010), 119902.

[18] L. Shen, J. Li, Equilibrium structure and strain energy of single-walled carbon nanotubes, *Phys. Rev. B* **71** (2005), 165427.

[19] F. H. Stillinger, T. A. Weber, Computer simulation of local order in condensed phases of silicon, *Phys. Rev. B*, **8** (1985), 5262–5271.

[20] J. Tersoff, New empirical approach for the structure and energy of covalent systems. *Phys. Rev. B*, **37** (1988), 6991–7000.

[21] M.M.J. Treacy, T.W. Ebbesen, J.M. Gibson, Exceptionally high Young's modulus observed for individual carbon nanotubes. *Nature* **381** (1996), 678–680.

[22] M.-F. Yu, B.S. Files, S. Arepalli, R.S. Ruoff, Tensile Loading of Ropes of Single Wall Carbon Nanotubes and their Mechanical Properties. *Phys. Rev. Lett.* **84** (2000), 5552–5555.

[23] T. Zhang, Z. S. Yuan, L. H. Tan, Exact geometric relationships, symmetry breaking and structural stability for single-walled carbon nanotubes, *Nano-Micro Lett.* **3** (2011), 4:28–235.

[24] X. Zhao, Y. Liu, S. Inoue, R. O. Jones, Y. Ando, Smallest carbon nanotibe is 3Å in diameter, *Phys. Rev. Lett.* **92** (2004), 12:125502.

E-mail address: `edoardo.mainini@unipv.it`

E-mail address: `murakawa@math.kyushu-u.ac.jp`

E-mail address: `paolo.piovano@univie.ac.at`

E-mail address: `ulisse.stefanelli@univie.ac.at`